Int. J. Electrochem. Sci., 14 **(2019)** 3408 – 3417, doi: 10.20964/2019.04.01

International Journal of
ELECTROCHEMICAL
SCIENCE
www.electrochemsci.org

Enhanced High-Rate and Low-Temperature Electrochemical Properties of $LiFePO_4$/Polypyrrole Cathode Materials for Lithium-ion Batteries

Yuan Gao[1,2,*], *Kun Xiong*[1], *Hui Xu*[1], *Bingfeng Zhu*[3]

[1] School of environment and resources, Engineering Research Center for Waste Oil Recovery Technology and Equipment of Ministry of Education, Chongqing Technology and Business University, Chongqing 400040, China
[2] Department of Chemistry, University at Albany, State University of New York, Albany, NY 12222, USA
[3] Chongqing Occupational Disease Prevention Hospital, Chongqing 400040, China
[*]E-mail: gaogone113117@ctbu.edu.cn

Received: 14 December 2018 / *Accepted:* 22 January 2019 / *Published:* 10 March 2019

Uniformly coated $LiFePO_4$/polypyrrole ($LiFePO_4$/PPy) composites were successfully prepared by in situ chemical oxidative polymerization. The structure and morphology of the composites were characterized by XRD, TG, FE-SEM and HRTEM. The results showed that the PPy layer coated on the $LiFePO_4$ particles is approximately 5 nm thick and forms a regular strip on the surface. The well-coated PPy can enhance the electronic conductivity and Li^+ diffusion velocity of $LiFePO_4$, resulting in improvement of the electrochemical performance of cathode materials. The charge/discharge test results showed that the optimized 2.95% PPy-coated $LiFePO_4$/PPy composites exhibited excellent specific capacity, rate capability and low-temperature performance. The $LiFePO_4$/PPy cathodes showed initial specific capacities of 153 mAh/g, 138 mAh/g and 118 mAh/g at 0.1 C, 1 C and 5 C, respectively. Moreover, the initial discharge capacities at 0.1 C, 0.5 C, and 1 C were 128, 106.5 and 85.7 mAh/g, respectively, at -20 °C.

Keywords: Lithium-ion battery; Lithium iron phosphate; Coating; Polypyrrole; Low temperature

1. INTRODUCTION

Olivine-structured lithium iron phosphate ($LiFePO_4$) has been investigated as a cathode material for lithium ion batteries due to its high theoretical capacity (170 mAh/g), flat voltage profile, low price, nontoxicity and ecofriendliness [1-3]. Nevertheless, the two major disadvantages of poor

electronic conductivity and low Li^+ diffusion restrict the use of this material in high-rate applications [4,5], leading to the inability to replace commercialized $LiCoO_2$ in the field of high-energy batteries. In recent years, some research efforts have been devoted to overcoming these problems by element doping [6-8], surface modification [9-11], particle size reduction and crystal surface optimization [12-14].

Recent studies reported [15,16] that Ru-doped and Ni-Co-Mn-doped $LiFePO_4$/C displayed outstanding electrochemical performance because the diffusion rate of Li^+ and the electrochemical conductivity of cathode materials were promoted by doping. Peng et al [17] synthesized facet-controlled 2D $LiMPO_4$ (M = Mn, Fe, Co) nanosheets with significantly large exposure of (010) facets, which shortened the pathway of Li^+ diffusion and provided a high proportion of effective surface for Li^+ extraction/insertion. The as-prepared $LiFePO_4$ nanosheets have thus demonstrated an improved rate capability, with a specific capacity of ~80 mAh/g at a high rate of 30 C.

Surface modification has been extensively studied as one of the most convenient methods to increase the electrical conductivity of $LiFePO_4$ and increase the rate capability of electrode materials. Chen et al [18] prepared RGO-coated $LiFePO_4$/C composites ($LiFePO_4$/C@G) by using a sol-gel method. The growth of $LiFePO_4$ particles was restrained by such surface modification; furthermore, the electronic conductivity of the $LiFePO_4$ electrode materials was improved.

Recently, some researchers have found that organic polymers have many advantages as modified materials, such as excellent electronic conductivity, ease of constructing three-dimensional conductive frameworks and porous structures, which are beneficial for Li^+ extraction/insertion [19-21]. PPy has been intensively investigated as an electrode material because of its high electronic conductivity (10^2～10^3 S/cm) and theoretical specific capacity of 72 mAh/g [22]. In addition, PPy was facilely fabricated and doped [23-24]. Modification of $LiFePO_4$ by conductive PPy can not only replace carbon as a conductive agent but also improve the conductive capability, cycling performance and low-temperature electrochemical properties of $LiFePO_4$ [25].

In our previous works, well-shaped $LiFePO_4$ nanorods were obtained through the solvothermal method. $LiFePO_4$ nanorods exhibited good conductivity and excellent electrochemical properties by reducing the crystal size along the *b* axis, thus shortening the diffusion path of Li^+ extraction/insertion. We hope that the conductivity of $LiFePO_4$ nanorods can be further enhanced by surface modification to increase the performance of these materials.

In this paper, PPy-modified $LiFePO_4$ nanorod composite materials were synthesized through in situ chemical oxidative polymerization. The morphology and structure of the $LiFePO_4$/PPy composite materials were studied. The electrochemical performance of the prepared $LiFePO_4$/PPy composite was evaluated from room temperature to -20 °C.

2. MATERIALS AND METHODS

2.1 Materials preparations

$LiFePO_4$/PPy nanorod composites were synthesized through in situ chemical oxidative polymerization. $C_{21}H_{21}FeO_9S_3 \cdot 6H_2O$ was first dissolved in 30 ml deionized water and stirred for 30

min at room temperature, followed by addition of 1 g $LiFePO_4$ nanorod powder (synthesized in a previous work [26]). Second, pyrrole monomers were dropped into the above mixed precursor solution with continued stirring for 18 h. The molar ratio of oxidant to monomer is 3:1. The powders were collected by vacuum filtration, washed with deionized water and absolute ethyl alcohol and dried at 100 ℃. Additionally, the amount of pyrrole monomers was 0 µl, 30 µl, 60 µl, 120 µl and 180 µl. The $LiFePO_4$/PPy composites were named a, b, c, d, and e, respectively.

2.2 Materials characterization

The phase purity of the prepared samples was determined by X-ray diffraction (MO3xHF22, MacScience, Japan). The coating amount of PPy was determined by a TG analyser (SDT Q600, TE) in an oxygen atmosphere. Field emission scanning electron microscopy (JSM 6701, JEOL) and high-resolution transmission electron microscopy (JEM 2100F, JEOL) were used to characterize the surface morphology of the samples.

2.3 Electrochemical characterization

The prepared $LiFePO_4$/PPy composites were assembled into simulated batteries for electrochemical performance testing. The working electrode was mixed with active material, acetylene black and adhesive (polyvinylidene fluoride) at a mass ratio of 85:7:8. Mixed positive paste was coated on aluminium foil and dried under a vacuum for 24 h. Then, 1 M LiPF6 dissolved in an EC and DEC (1:1, v/v) mixture solution was used as an electrolyte. All cells were assembled in an argon-filled glove box. Xinwei (BTS-5V3A) was used for the battery charging/discharging test between 2.5 V and 4.2 V. A Solartron Analytical 1287+1260 Electrochemical Workstation (AMETEK Company) was used for electrochemical impedance spectroscopy (EIS) measurements. The test conditions were set to +5 mV AC disturbance signals and frequencies ranging from 10^{-2} Hz to 10^5 Hz.

3. RESULTS AND DISCUSSION

3.1 XRD analysis

Typical XRD patterns of pure $LiFePO_4$ and PPy-modified $LiFePO_4$ samples are presented in Fig. 1. The XRD diffraction patterns of five samples are consistent with the olivine structure (JCPDS No. 40-1499) indexed by orthorhombic Pnma, indicating that the method of in situ chemical oxidative polymerization does not significantly change the structure of $LiFePO_4$. In addition to the diffraction peaks from $LiFePO_4$, however, both d and e show new diffraction peaks at 18.0° and 30.8°, which are indexed to $FePO_4$ as impurity phases (JCPDS No. 37-0478). This indicates that the excess oxidant results in the formation of $FePO_4$ under the conditions of in situ chemical oxidative polymerization [27]. No characteristic diffraction peaks of PPy were detected, indicating that PPy existed in an amorphous state.

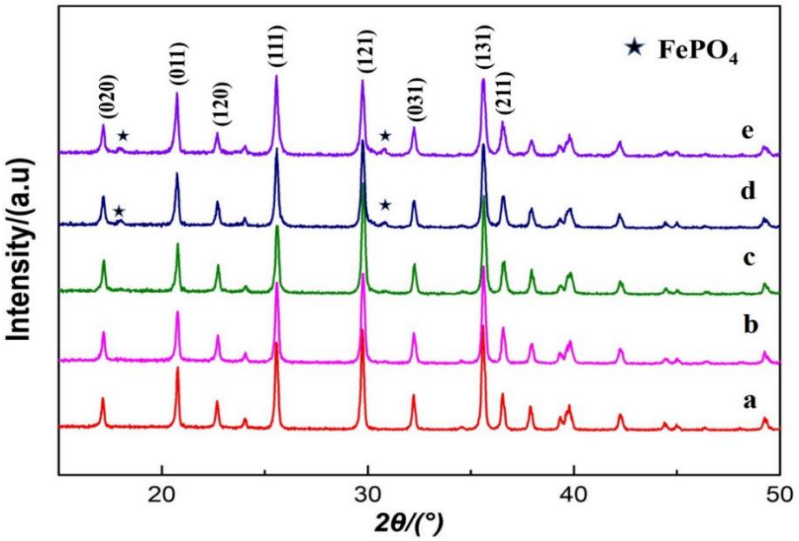

Figure 1. XRD patterns of samples (a) $LiFePO_4$ without PPy, (b) $LiFePO_4$/PPy (30 µl), (c) $LiFePO_4$/PPy (60 µl), (d) $LiFePO_4$/PPy (120 µl) and (e) $LiFePO_4$/PPy (180 µl)

3.2 PPY coating amount analysis

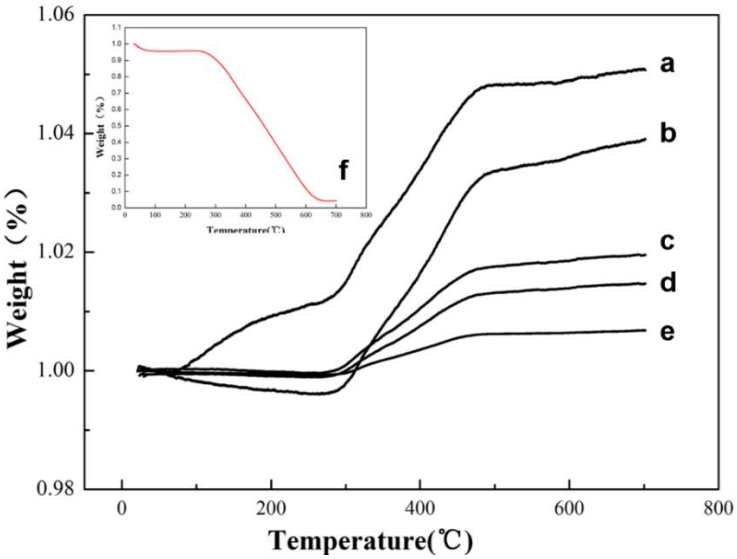

Figure 2. TGA curves of (a) $LiFePO_4$, (b) $LiFePO_4$/PPy (30 µl), (c) $LiFePO_4$/PPy (60 µl), (d) $LiFePO_4$/PPy (120 µl), (e) $LiFePO_4$/PPy (180 µl) and (f) PPy

TGA curves of composite samples and PPy are presented in Fig. 2. Curve (f) shows that PPy has been completely degraded at 700℃. Curve (a) is the weight change curve of $LiFePO_4$ in an oxygen atmosphere. The final weight of $LiFePO_4$ increased by 5.07 wt.% [28]. TGA curves of $LiFePO_4$/PPy composites (b, c, d, e) with different pyrrole monomers (30 µl, 60 µl, 120 µl, 180 µl) were obtained. Considering the oxidation reaction and PPy degradation, the coating amounts of PPy were 1.16%, 2.95%, 3.60%, and 4.39%. From the coating amount of PPy, it can be concluded that the addition of

pyrrole monomer is not directly proportional to the increase in the coating amount because of the oily nature of pyrrole.

3.3 morphology analysis

The TEM image of $LiFePO_4$/PPy displayed in Fig. 3 (a) confirms that the particles exist as highly crystalline nanorods. After coating the PPy (2.95%) by in situ polymerization, the morphology of the $LiFePO_4$ nanorods has not changed, and the particles are connected on the amorphous polypyrrole to form a conductive three-dimensional network connection. We can see (Fig. 3 c) that the surface of the $LiFePO_4$ particles is coated with a regular PPy strip with a thickness of approximately 5 nm. The suitable polypyrrole layer on the surface of $LiFePO_4$ offers a channel for electron transport and effectively improves the electronic conductivity of the material.

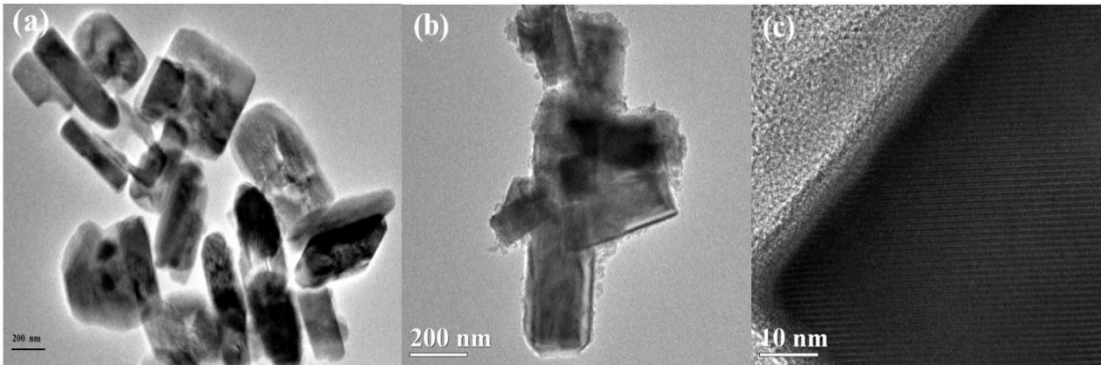

Figure 3. (a) TEM images of $LiFePO_4$, (b) TEM and (c) HRTEM images of $LiFePO_4$/PPy

3.4 Electrochemical characteristics

Fig. 4 (a) exhibits the discharge curves of $LiFePO_4$ without and with various contents of PPy coating between 4.2 V and 2.5 V at 0.1 C (1 C =170 mAh/g). Compared with pure $LiFePO_4$, PPy-coated $LiFePO_4$ exhibits a higher discharge capacity. The 2.95% PPy-coated LFP cathode (c) has a maximum specific discharge capacity of 153 mAh/g and a constant discharge voltage, suggesting a lower polarization of the electrode. The well-coated PPy can connect $LiFePO_4$ particles and form a good conductive network between particles, resulting in an improvement in electronic conductivity. When the amount of PPy is small, the polymer cannot completely coat the $LiFePO_4$ particles, and the improvement in the conductivity of the material is limited. With an increasing amount of PPy, we can see that the discharge capacities of $LiFePO_4$/PPy (3.60%) and $LiFePO_4$/PPy (4.39%) are reduced to 138 mAh/g and 130 mAh/g at 0.1 C, and the discharge plateau declines. The discharge specific capacity of PPy itself is small (72 mAh/g), and the excessive coating of low-specific-capacity PPy reduces the discharge specific capacity of the cathode material. Furthermore, too much PPy will prevent Li^+ extraction/insertion during charging and discharging. In addition, PPy has no stable

discharge voltage platform, which will inevitably affect the discharge platforms of $LiFePO_4$/PPy composites.

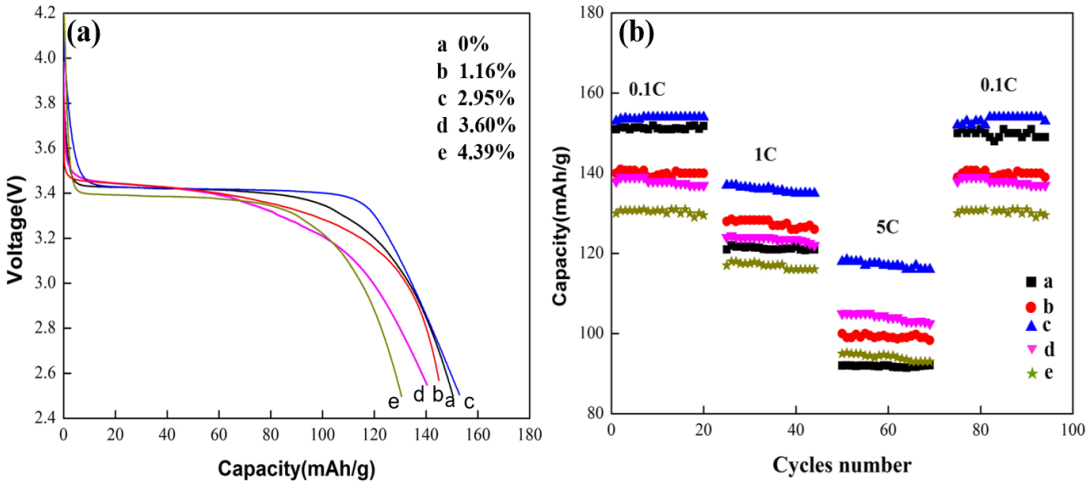

Figure 4. (a) Typical discharge curves of $LiFePO_4$/PPy with different contents of PPy at 0.1 C, (b) The cyclic performance of $LiFePO_4$/PPy with different contents of PPy at various rates

Table 1. Comparison of the electrochemical performance of the $LiFePO_4$ composite cathode modified with different conductive materials at room temperature.

sample	rate/specific capacity (mAh/g)	rate/specific capacity (mAh/g)	ref.
LFP/C microparticles	0.1 C/162.7	5 C/109.4	[29]
LFP/C nanocrystalline	0.1 C/162	5 C/108.6	[30]
LFP/C-V_2O_3 (0.5 mol%)	0.1 C/149	5 C/108	[31]
LFP/MWCNT (10 wt.%)	0.1 C/150	5 C/102.5	[32]
LFMP/RGO	0.1 C/148	5 C/60	[33]
LFP/C/3%PTPAn	0.1 C/149.6	5 C/113	[34]
$LiFePO_4$/PPy	0.1 C/153	5 C/118	This work

Fig. 4 (b) displays the cyclic reversibility of $LiFePO_4$/PPy cathodes with different contents of PPy at various rates. $LiFePO_4$/PPy cathodes with a coating amount of 2.95% show outstanding cyclic reversibility without obvious capacity fading, and after 20 cycles, the capacity fading rate is 1.2%. Even at a 5 C current density, the $LiFePO_4$/PPy (2.95%) can still maintain a stable flat discharge voltage plateau of more than 3 V and deliver a discharge capacity of 118 mAh/g. In contrast, the $LiFePO_4$ without PPy yields only 95 mAh/g at 5 C. The test results suggest that the discharge specific

capacities of all $LiFePO_4$/PPy cathode materials are higher than that of the uncoated sample at 5 C, which indicates that the electronic conductivity of $LiFePO_4$ could be improved by PPy coating and that the electrochemical performance of $LiFePO_4$ is improved significantly at higher current density. The specific capacity and rate capability of the $LiFePO_4$/PPy composites presented in this work are superior or comparable to those of the LFP composite cathode modified with different conductive materials in previous studies (Table 1).

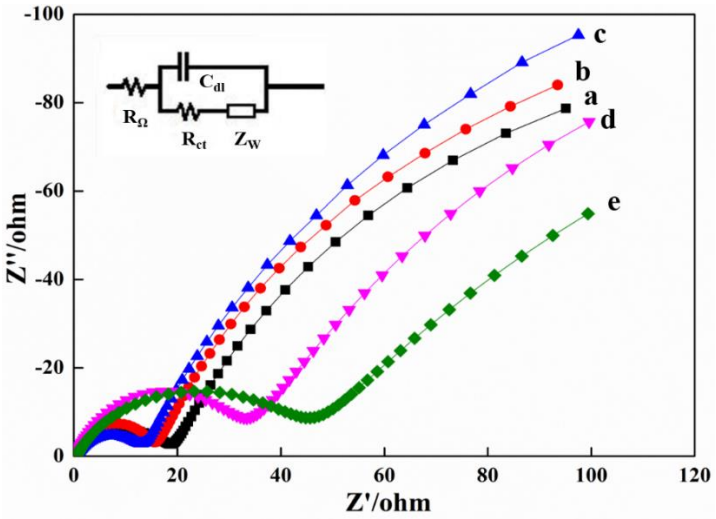

Figure 5. Electrochemical impedance spectra of $LiFePO_4$/PPy with different contents of PPy.

electrochemical impedance spectroscopy (EIS) was used to analyse the influence of PPy coating on the electrochemical properties of $LiFePO_4$/PPy. Fig. 5 shows the EIS curves of the $LiFePO_4$/PPy electrodes with different contents after three cycles at full charge. The EIS curves indicate an intercept at high frequency, corresponding to the ohmic resistance (R_Ω) of the electrolyte and electrode; a depressed semicircle in the medium frequency region, corresponding to charge transfer (R_{ct}) at the $LiFePO_4$ cathode electrolyte interface; and a straight line at low frequencies, related to the Warburg impedance (Z_w), which results from the diffusion of Li^+ in the bulk of the electrode material [35].

Table 2. Impedance parameters of $LiFePO_4$/PPy with different contents of PPy electrodes (fully discharged) at 278 K.

$LiFePO_4$/PPy	R_Ω/Ω	R_{ct}/Ω	σ	D_{Li} (cm^2/s)
a (0%)	0.46	18.78	39.54	6.605×10^{-12}
b (1.16%)	0.49	15.81	36.56	7.094×10^{-12}
c (2.95%)	0.51	12.97	31.21	1.061×10^{-11}
d (3.60%)	0.38	33.46	34.81	7.825×10^{-12}
e (4.39%)	0.52	45.65	44.73	4.739×10^{-12}

Table 2 shows the parameters of the equivalent circuit used for simulations. It is obvious that $LiFePO_4$/PPy cathodes with a coating amount of 2.95% exhibit the lowest charge transfer resistance of 12.97 Ω and the highest Li^+ diffusion coefficient of 1.061×10^{-11} cm^2/s. The smaller charge transfer resistance and the higher Li^+ diffusion coefficient indicate the more feasible transfer of Li^+ and electrons on the electrode, which is beneficial for overcoming the restriction of kinetics in the charge/discharge process and improving the low-temperature performance of the material. These findings may be attributed to the suitable conductive PPy layer on the surface of $LiFePO_4$, which provides excellent electron and ion transport channels. As shown in Table 1, the value of R_Ω is negligible in comparison with that of R_{ct}.

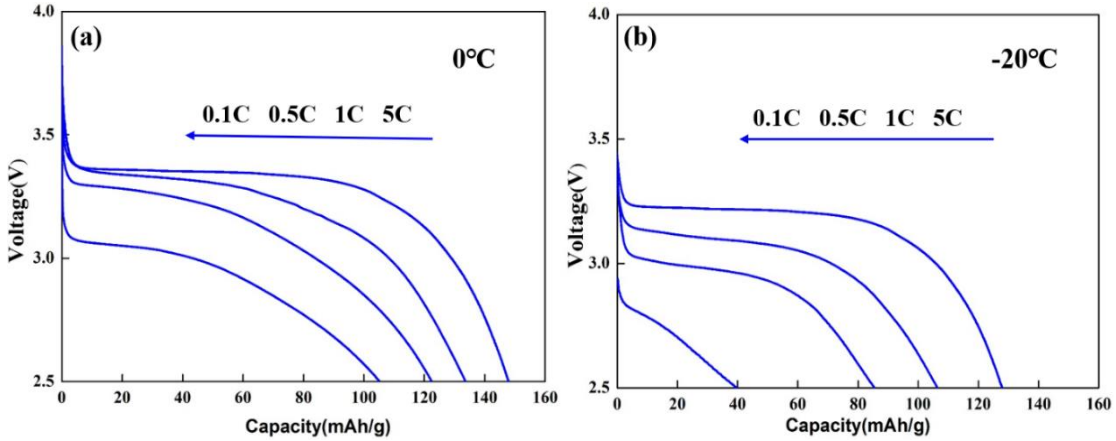

Figure 6. Typical discharge curves of $LiFePO_4$/PPy with a coating amount of 2.95% under various rates at (a) 0 °C and (b) -20 °C.

The excellent electrochemical performance at low temperature is an important parameter for the application of a material in EVs and HEVs [36]. The electrochemical measurement was also carried out at a lower temperature. Fig. 6 (a) shows the discharge specific capacity of $LiFePO_4$/PPy with a coating amount of 2.95% at 0 °C. The specific capacity of $LiFePO_4$/PPy can still reach 148, 133.7, 122.5 and 105.2 mAh/g at rates of 0.1 C, 0.5 C, 1 C, and 5 C, respectively, at 0 °C. Even at the lower temperature of -20 °C, the $LiFePO_4$/PPy cathode delivers a high discharge capacity of 128, 106.5 and 85.7 mAh/g at rates of 0.1 C, 0.5 C, and 1 C, respectively.

Fig. 7 displays the cyclic reversibility of $LiFePO_4$/PPy with a coating amount of 2.95% cathodes under various rates at 0°C and -20°C. At low temperature, the $LiFePO_4$/PPy cathodes show satisfactory cyclic performances, with the capacity decreasing by less than 1.5% after 10 cycles at various rates. The superior low-temperature performance of the $LiFePO_4$/PPy material can be attributed to the better conductive polymer coating layer, which can enhance the ionic and electronic conduction in the electrode.

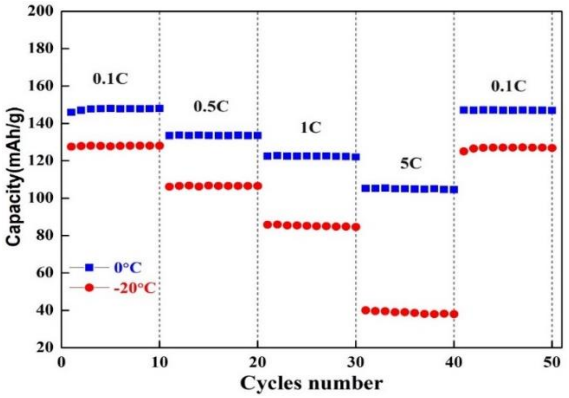

Figure 7. The cyclic performance of $LiFePO_4$/PPy with a coating amount of 2.95% at various rates at 0°C and -20°C.

4. CONCLUSION

Uniformly coated $LiFePO_4$/PPy nanorod composites were successfully obtained by in situ chemical oxidative polymerization. Appropriate in situ coating polymerization will not change the structure or morphology of the $LiFePO_4$ nanorods. Particles are connected on the amorphous PPy to form a conductive three-dimensional network connection. A suitable PPy layer with a thickness of 5 nm on the surface of $LiFePO_4$ provides a pathway for electron transport and effectively improves the electronic conductivity of the material. Uniformly coated $LiFePO_4$/PPy cathode materials exhibited excellent specific capacity, high-rate capability and low-temperature performance.

ACKNOWLEDGEMENTS
This research work was sponsored by the National Natural Science Foundation of China (Grant No.: 201606028), by the Science and Technology Project from Chongqing Education Commission (Grant No.: KJ1600630), and by the Scientific Research Foundation of Chongqing Technology and Business University (1856022).

References

1. A.K. Padhi, K.S. Nanjundaswamy and J.B. Goodenough, *J. Electrochem. Soc*., 144 (1997) 1188.
2. G. Amold, J. Garche, R. Hemmer, S. Strobele, C. Vogler and M. Wohlfahrt-Mehrens, *J. Power Sources*, 247 (2003) 119.
3. K. Hirose, Y. Benino and T. Komatsu, *Solid State Ionics,* 178 (2007) 801.
4. X.R. Sun, J.J. Li, C.S. Shi, Z.Y. Wang, E.Z. Liu, C.N. He, X.W. Du and N.Q. Zhao, *J. Power Sources*, 220 (2012) 264.
5. S.Y. Chung, J.T. Bloking and Y.M. Chiang, *Nat. Mater*., 1 (2002) 123.
6. A. Paolella, G. Bertoni, P. Hovington, Z. Feng, R. Flacau, M. Prato, M. Colombo, S. Marras, L. Manna and S. Turner, *Nano Energy*, 16 (2015) 256.
7. C. Gao, J. Zhou, G.Z. Liu, L. Wang, *J Alloys Compd.*, 727 (2017) 501.
8. AR. Madram and M. Faraji, *New J Chem*., 41(2017)12190.
9. C. Wang, Z. Guo, W. Shen, Q. Xu, H. Liu and Y. Wang, *Adv. Funct. Mater*., 24 (2014) 5511.
10. E. Avci, M. Mazman, D. Uzun, E. Biçer and T. Sener, *J. Power Sources*, 240 (2013) 328.
11. C.C. Yang, Y.H. Hsu, J.Y. Shih, Y.S. Wu, C. Karuppiah, T.H. Liou and S.J. Jessie Lue, *Electrochim.*

Acta, 258 (2017) 773.
12. Z. Lu, H. Chen, R. Robert, B.Y.X. Zhu, J. Deng, L. Wu, C.Y. Chung and C.P. Grey, *Chem. Mater*., 23 (2011) 2848.
13. R. Martins, R. Goncalves, C.M. Costa, S. Ferdov and S. Lanceros-Méndez, *Nano-Structures & Nano-Objects,* 11 (2017) 82.
14. C. Nan, J. Lu, L. Li, L. Li, Q. Peng and Y. Li, *Nano Res*., 6 (2013) 469.
15. Y. Gao, L. Li, H. Peng and Z.D. Wei, *Chemelectrochem*, 12 (2014) 2146.
16. W.M. Liu, Q.L. Liu, M.L. Qia, L. Xu and J.Y. Deng, *Electrochim. Acta*, 257 (2017) 82.
17. L.L. Peng, X. Zhang, Z.W. Fang, Y. Zhu, Y.Y. Xie, Judy J. Cha and G.H. Yu, *Chem. Mater*., 29 (2017) 10526.
18. M.H. Chen, K.C. Kou, M.W. Tu, J. Hu, X.W. Du and B.S. Yang, *Solid State Ionics*, 310 (2017) 95.
19. K. Zaghib, K. Striebel, A. Guerfi, J. Shim, M. Armand and M. Gauthier, *Electrochim. Acta,* 50 (2004) 263.
20. D.C´ıntora-J´uarez, C.P´erez-Vicente, S. Ahmad and J.L. Tirado, *RSC Adv*., 4 (2014) 26108.
21. K. Zaghib, P. Charest, A. Guerfi, J. Shim, M. Perrier and K. Striebel, *J. Power Sources*, 146 (2005) 380.
22. Y.S. Cohen, M.D. Levi and D. Aurbach, *Langmuir*, 19 (23) (2003) 9804.
23. F.T.A. Vork, B.C.A.M. Schuermans and E. Barendrecht, *Electrochim. Acta*, 35 (1990) 67.
24. L. Wang, X. Li and Y. Yang, *React Funct Polym*., 47 (2001) 125.
25. D. Lepage, C. Michot and G. Liang, *Angew Chem Int* Ed., 50 (30) (2011) 6884.
26. Y. Gao, C. Ke, H.M. Chen, X.H. Hu, Z.H. Deng and Z.D. Wei, *J Energy Chem.*, 26 (3) (2017) 564.
27. W.M. Chen, Y.H. Huang and L.X. Yuan, *J Electroanal Chem*., 660 (1) (2011)108.
28. J. Chen and M. Whittingham, *Electrochem Commun.,* 8 (5) (2006) 855.
29. X.J. Ma, L.G. Gai and Y. Tian, *Int. J. Electrochem. Sci.,* 13 (2018) 1376.
30. J. Wang, Y.J. Gu, W.L. Kong, H.Q. Liu, Y.B. Chen and W. Liu, *Solid State Ionics,* 327 (2018) 11.
31. Y. Zhang, G.J. Shao, Z.P. M, G.L. Wang and J.P. Du, *Ionics,* 19 (2013) 1091.
32. C.L. Gong, Z.G. Xue, X.E. Wang, X.P. Zhou, X.L. Xie and Y.W. Mai, *J. Power Sources*, 246 (2014) 260.
33. C.A. Rossouw, K. Raju, H.T. Zheng and K.I. Ozoemena, *Applied Physics A*, 123 (2017) 769.
34. C. Su, Q.F. Huang, L.H. Xu and C. ZHang, *Acta Phys.-Chim. Sin.,* 30 (2014) 88.
35. Y. Kadoma, J.M. Kim, K. Abiko, K. Ohtsuki, K. Ui and N. Kumagai, *Electrochim. Acta*, 55 (2010) 1034.
36. M. Armand and J.M. Tarascon, *Nature*, 451 (2008) 652.